



## Singular bifurcations and regularization theory

Alexander Farutin and Chaouqi Misbah 

*Université Grenoble Alpes, CNRS, LIPhy, F-38000 Grenoble, France*

 (Received 25 February 2024; accepted 6 June 2024; published 27 June 2024)

Nonlinear sciences are present today in almost all disciplines, ranging from physics to social sciences. A major task in nonlinear science is the classification of different types of bifurcations (e.g., pitchfork and saddle-node) from a given state to another. Bifurcation analysis is traditionally based on the assumption of a regular perturbative expansion, close to the bifurcation point, in terms of a variable describing the passage of a system from one state to another. However, it is shown that a regular expansion is not the rule due to the existence of hidden singularities in many models, paving the way to a new paradigm in nonlinear science, that of singular bifurcations. The theory is first illustrated on an example borrowed from the field of active matter (phoretic microswimmers), showing a singular bifurcation. We then present a universal theory on how to handle and regularize these bifurcations, bringing to light a novel facet of nonlinear sciences that has long been overlooked.

DOI: [10.1103/PhysRevE.109.064218](https://doi.org/10.1103/PhysRevE.109.064218)

### I. INTRODUCTION

Nonlinear sciences have now become a common topic across different disciplines from physics and biology to social sciences [1]. An important goal of nonlinear sciences is to classify the number and nature of bifurcations. The lack of analytical solutions for nonlinear systems had led to a systematic development of perturbative schemes for centuries.

The classical theory of bifurcations has known its glory on chemical and physical systems. Typical examples are Bénard convection [2,3], Turing patterns [4–6], crystal growth [7–9], and so on. When varying a control parameter (e.g., temperature gradient in convection) the system exhibits a bifurcation from one state (e.g., quiescent fluid) into a new state (the fluid shows convection rolls) when the control parameter reaches a critical value. In particular, pitchfork bifurcations describe spontaneous symmetry breaking in many dynamical systems. If  $\mu$  designates the distance of the control parameter from the bifurcation point for a classical pitchfork bifurcation, then the amplitude  $A$  of the field describing the loss of symmetry, say, convection amplitude, behaves as  $A \sim \pm\mu^{1/2}$  for  $\mu > 0$ . The evolution equation of the amplitude  $A$  in the vicinity of the bifurcation point, known as normal form, reads for a supercritical pitchfork bifurcation

$$\dot{A} = \mu A - A^3, \quad (1)$$

where dot designates derivative with respect to time  $t$ . The steady-state solutions of (1) are  $A = 0$  for  $\mu < 0$  (stable branch) and  $A = 0$  (unstable) and  $A = \pm\mu^{1/2}$  (stable) for  $\mu > 0$ . More generally, pitchfork bifurcations correspond to solutions  $A(\mu)$  of a steady-state problem,

$$AF(A, \mu) = 0, \quad (2)$$

where the function  $F(A, \mu)$  describing the physics of the problem satisfies the symmetry condition in A:

$$F(-A, \mu) = F(A, \mu) \quad (3)$$

and  $F(A = 0, \mu = 0) = 0$ . The majority of physically relevant problems are so complex that the function  $F(A, \mu)$ , let alone the set of solutions  $A(\mu)$  of Eq. (2), cannot be calculated exactly. In this case, the problem has to be either solved numerically or perturbatively. In the latter case, the function  $F$  is expanded in a power series of  $A$ ,

$$F(A, \mu) = \sum_{k=0}^{\infty} a_k(\mu)A^{2k}, \quad (4)$$

in which several first coefficients  $a_k(\mu)$  can be calculated exactly or approximated numerically for many important problems. The series (4) can be truncated at the second term for  $A$  sufficiently small, which, after an appropriate rescaling of  $A$  and  $\mu$ , can be substituted in (2) to produce the steady-state form of Eq. (1).

Expansion (4) requires the function  $F(A, \mu)$  to be analytical in some region around  $A = 0$ . While this is often the case, there are problems in which this assumption fails. A notable example comes from the field of active matter, a subject of great topicality: It has been shown by analytical calculations that the swimming velocity of autophoretic particles scales linearly with the control parameter close to the critical point separating the stationary and motile states [10–12]. In its simplest version, an autophoretic particle consists of a droplet either emitting or absorbing a solute which diffuses and is advected in the suspending fluid [10,13–20]. The solute molecules modify the surface tension of the droplet, which can induce fluid flows around the droplet due to Marangoni stresses at the droplet-fluid interface. For low-enough emission rate, the particle is stationary and the solute concentration in the fluid depends only on the distance from the droplet

\*Contact author: [chaouqi.misbah@univ-grenoble-alpes.fr](mailto:chaouqi.misbah@univ-grenoble-alpes.fr)

center. If the emission or absorption rate exceeds a critical value, then the particle transits from a nonmotile to a motile state, in which the concentration field is polarized along the particle surface. This concentration polarity leads to the swimming of the particle, while the backward flow of fluid in the reference frame comoving with the particle maintains the concentration polarity.

This transition clearly represents a spontaneous symmetry breaking, since the stationary state is completely rotationally invariant with respect to the droplet center and the swimming direction is not predefined. Such transitions are classically described by pitchfork bifurcations, with the instability amplitude scaling as  $A = \pm\mu^{1/2}$  for  $\mu > 0$ . However, the amplitude of the swimming velocity was found to behave (for infinite system size) [10–12] as  $|A| \sim \mu$  (or  $A \sim \pm\mu$ ,  $\mu > 0$ ), which cannot be obtained from a classical pitchfork bifurcation. This suggests a normal form,

$$\dot{A} = \mu A - A|A|, \quad (5)$$

in a marked contrast with the classical picture represented by (1). On the other hand, numerical simulations [16] of this system are consistent with a classical pitchfork bifurcation,  $A \sim \pm\mu^{1/2}$ . Furthermore, a classical pitchfork bifurcation is found in analytical calculations of a two-dimensional (2D) model of autophoretic particles [21,22].

The first motivation of this work is to explain these contradictory results. To this end, we introduce a notion of singular pitchfork bifurcation, for which the function  $F(A, \mu)$  in Eq. (2) is an analytic function of complex amplitude  $A$  with a singular point at  $A = 0$  [where  $|A|$  corresponds to  $(A^2)^{1/2}$ , which has a branch point for  $A = 0$ ]. We show that singular bifurcations can be regularized by moving the singular point  $A = 0$  along the imaginary axis, which produces a classical pitchfork bifurcation. For example, the function  $|A|$  can be regularized as  $(A^2 + \epsilon^2)^{1/2}$ , where  $\epsilon$  is the regularization parameter. The function  $(A^2 + \epsilon^2)^{1/2}$  has a regular Taylor expansion for  $A = 0$  and tends to  $|A|$  as  $\epsilon$  decreases to 0. We argue that the transition of autophoretic particles to motility in an infinite fluid occurs via a singular pitchfork bifurcation, which is regularized for finite system size, used in analytical 2D calculations or by discretization in full numerical simulation. Another way to regularize the problem is by introducing consumption of the solute in the fluid suspending the particle. This analysis is performed using a simplified model of autophoretic particles, which has an explicit solution and reproduces qualitatively the transition to motility.

The second question considered in this work is how the singular limit can be reconstructed from the perturbative expansion of the regularized problem, which is the only information that can be obtained by analytical calculation for many systems. First, we show that the radius of convergence of the perturbative expansion of the regularized problem at  $A = 0$  tends to 0 in the singular limit. This puts mutually exclusive requirements on the regularization parameter, which has to be both small enough to approach the singular limit and large enough to ensure the convergence of the perturbative solution in a reasonable region of  $A$ . As a consequence, the perturbative expansion of the regularized problem does not, in general, give a good approximation of the singular limit at any range of  $A$  or  $\epsilon$ . To solve this problem, we propose a

change of variables which allows us to reconstruct the singular limit from the several first terms of the perturbative expansion of the regularized problem. The reconstruction converges to the exact result as more and more terms of the perturbative expansion are taken into account, as shown for some examples. In the simplest case, the reconstruction is exact. This reconstruction can also be used to approximate the regularized problem beyond the radius of convergence of the perturbative series.

## II. A BRIEF PRESENTATION OF A PHORETIC MODEL WITH SINGULAR BIFURCATION

It is instructive to begin with an explicit model revealing a singular bifurcation. We first recall the full model, before considering a simplified version which can be handled fully analytically. The model consists [14] of a rigid particle (taken to be a sphere with radius  $a$ ), which emits or absorbs a solute that diffuses and is advected by the flow. The advection-diffusion equations read

$$\frac{\partial c}{\partial t} + \mathbf{u} \cdot \nabla c = D\Delta c, \quad (6)$$

where  $c$  is the solute concentration and  $D$  is the diffusion constant. The velocity field  $\mathbf{u}$  is obtained by solving Stokes equations in the fluid suspending the particle. The associated boundary conditions of surface activity and the swimming velocity are

$$D\mathbf{n}(\mathbf{r}) \cdot \nabla c(\mathbf{r}, t) = -\mathcal{A} \quad (7)$$

for the solute emission and

$$\mathbf{u}(\mathbf{r}, t) = \mathbf{V}_0(t) + \mathcal{M}\nabla^s c(\mathbf{r}, t) \quad (8)$$

for the slip velocity at the particle boundary. Here  $\mathbf{n}$  is the unit normal;  $\mathbf{V}_0$  is the translational velocity of the particle, which will be taken to be along the  $z$  direction;  $\mathcal{A}$  is the emission rate ( $\mathcal{A} > 0$ : emission,  $\mathcal{A} < 0$ : adsorption); and  $\mathcal{M}$  is a mobility factor (which can be either positive or negative); see Ref. [14] for more details. The operator  $\nabla^s$  in (8) denotes the surface gradient. Equations (7) and (8) are valid at the boundary of the particle, while the boundary conditions at infinity are  $c = 0$  and  $\mathbf{u} = 0$ .

Assuming no external force acts on the particle, the swimming velocity can be related to the concentration distribution at the particle surface. For the axially symmetric concentration fields considered in this work, this relation has a simple expression in polar coordinates taking the particle center as the origin and the symmetry axis as the polar direction:

$$V_0(t) = -\frac{\mathcal{M}}{a} \int_{-1}^1 \cos(\theta)c(\theta, t)d\cos(\theta), \quad (9)$$

where  $\theta$  is the polar angle. The particle velocity  $V_0(t)$  in (9) is a signed projection of the velocity on the polar direction of the spherical coordinates. This model has been studied numerically [14,16,17], coming to the conclusion that when Péclet number,  $Pe$  (with  $Pe = |\mathcal{A}\mathcal{M}|a/D^2$ ), is sufficiently small the only solution is the nonmoving state of the particle, with a concentration field that is symmetric around the particle. When  $Pe$  exceeds a critical value it is shown that the

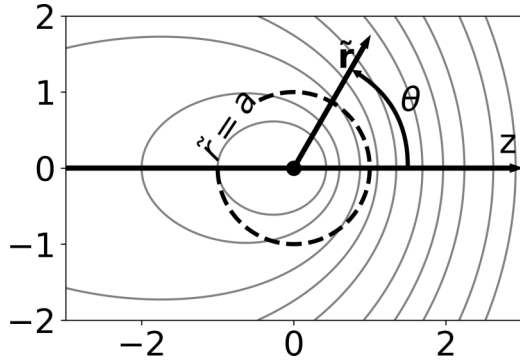


FIG. 1. Schematic view of the point-source model of an autophoretic particle. The vector  $\tilde{\mathbf{r}} = \mathbf{r} - \mathbf{V}_0 t$  measures the coordinates in comoving frame. Gray lines show concentration levels for a moving (in positive  $z$  direction) particle.

concentration field loses its spherical symmetry and a concentration comet develops, resulting in a motion of the particle with a constant velocity  $V_0$ . It is found numerically (for a 2D version of this model) [16] that  $V_0$  is well represented by  $V_0 \sim \sqrt{\text{Pe} - \text{Pe}_1}$ , where  $\text{Pe}_1$  is the critical value of  $\text{Pe}$  at which the transition from a nonmotile to a motile state occurs. The determination of the critical condition has also been analyzed by linear stability analysis [14,16,17]. Analytical asymptotic perturbative studies [10–12] (for an infinite system size) revealed that the velocity of the swimmer follows in fact the following singular behavior  $|V_0| \sim (\text{Pe} - \text{Pe}_1)$ .

### III. EXACTLY SOLVABLE MODEL

In order to understand the origin of this discrepancy, we use a simplified model of autophoretic particles, which has an explicit solution, while reproducing qualitatively the transition to motility. The model geometry and notations are shown schematically in Fig. 1. This model was introduced in Ref. [23] and studied by other authors [24,25]. The main simplification is to disregard the fluid, in that the variable  $\mathbf{u}$  is ignored in what follows. This simplification is valid if the particle size is small in comparison to length scales of interest. The only length scale is given by  $D/V_0$ , so this assumption corresponds to assuming  $a \ll D/V_0$ . Under this assumption the particle can be taken as a quasimaterial point so that  $c$  obeys (in the laboratory frame)

$$\frac{\partial c}{\partial t} - D\Delta c = S\delta(\mathbf{r} - \mathbf{V}_0 t), \quad (10)$$

where  $S$  is the emission rate [related to  $\mathcal{A}$ , by  $\mathcal{A} = S/(4\pi a^2)$ ].

Using the diffusion propagator the solution is given by

$$c(\mathbf{r}, t) = \int_0^\infty d\tau \frac{S}{(4\pi D\tau)^{3/2}} \exp\left\{-\frac{(\mathbf{r} + \mathbf{V}_0\tau - \mathbf{V}_0 t)^2}{4D\tau}\right\}, \quad (11)$$

Expression (11) can be integrated to yield

$$c(\mathbf{r}) = \frac{S}{4\pi D} \frac{\exp\left\{-\frac{\tilde{\mathbf{r}} \cdot \mathbf{V}_0 + |\mathbf{V}_0| \tilde{r}}{2D}\right\}}{\tilde{r}} \quad (12)$$

with  $\tilde{\mathbf{r}} = \mathbf{r} - \mathbf{V}_0 t$  (the coordinate in the frame attached to the particle). Along  $z$ , it is clear that the concentration decays

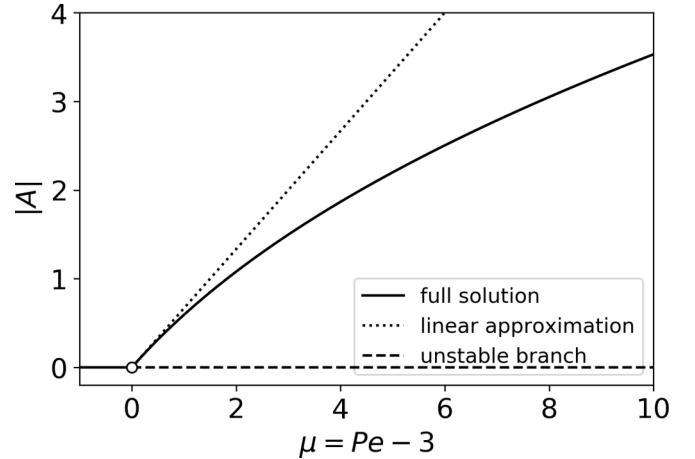


FIG. 2. Singular pitchfork bifurcation in the exactly solvable model of transition to motility for autophoretic particles.

exponentially with distance ahead of the particle, while it decays only algebraically at the rear ( $c$  has front-back asymmetry). Indeed, the emitted solute is advected (in the comoving frame) backwards, enriching the rear zone, whereas ahead of the particle only diffusion can be effective.

Using (9), only the first spherical harmonic enters the expression of velocity, and we obtain  $V_0 = -Mc_1/(a\sqrt{3\pi})$ ,  $c_1$  being the first harmonic amplitude, obtained by projection of (12) on that harmonic. This yields an implicit equation for  $V_0$ . We write this equation in nondimensional form,

$$A = 4\text{Pe} e^{-|A|/2} \left[ \frac{A \cosh(A/2) - 2 \sinh(A/2)}{A^2} \right], \quad (13)$$

where nondimensional velocity  $A \equiv \frac{aV_0}{D}$  serves as the amplitude being solved for and the Péclet number  $\text{Pe} = \mathcal{A}ma/D^2$  acts as the bifurcation parameter. Expanding for small  $A$  we obtain

$$A = \frac{\text{Pe}}{\text{Pe}_1} A(1 - |A|/2), \quad (14)$$

where  $\text{Pe}_1 = 3$ , is the critical Péclet number. In the full model with fluid flow it was found that the critical value is  $\text{Pe}_1 = 4$  [14]. Including hydrodynamics close to particle surface we can capture analytically this result (see Appendix A).

The result (14) has been also obtained in the full model with flow (where no analytical solution is known) thanks to a singular perturbative scheme [10–12]. The exact solutions of (13) and the linear approximation (14) are shown in Fig. 2. We see from (14) that  $A = 0$  always exists. When  $\text{Pe} > \text{Pe}_1$ , there exists another solution given by

$$|A| \simeq \frac{2}{3}\mu, \quad (15)$$

where  $\mu = \text{Pe} - \text{Pe}_1$  measures the distance from the critical point. Expression (15) corresponds to a pitchfork bifurcation (and not transcritical [11]), where the  $A = 0$  solution becomes unstable in favor of two symmetric solutions,  $A \propto \pm\mu$  for  $\mu > 0$ . This is, however, an atypical behavior of a pitchfork solution and is traced back to the infinite system size (as seen below). We refer to this bifurcation as *singular pitchfork*

*bifurcation*. The term “singular” refers to the nonanalytic nature of Eq. (13), from which  $A$  is calculated.

We found that finite domain regularizes Eq. (13) and turns the singular bifurcation into a classical pitchfork bifurcation (see Appendix B). Another way to regularize the model is via a consumption of solute in the bulk [24]. In that case we modify Eq. (10) by adding  $\beta c$  on the left-hand side, where  $\beta$  is the consumption rate. We have in mind the possibility that the emitted solute is consumed by a chemical reaction in the bulk. The modified model is solved by multiplying the expression under the integral in Eq. (11) by the decay factor  $e^{-\beta\tau}$  [where  $\tau$  is a dummy variable of integration in Eq. (11)]. The equation for  $A$  becomes

$$A = 4Pe e^{-\sqrt{A^2 + \epsilon^2}/2} \left[ \frac{A \cosh(A/2) - 2 \sinh(A/2)}{A^2} \right] \quad (16)$$

with  $\epsilon^2 = 4a^2\beta/D$ . For  $\epsilon = 0$  we recover the singular bifurcation equation (13), and for  $\epsilon \neq 0$  we obtain a regular pitchfork bifurcation. Expansion for small  $A$  provides

$$A = Pe a e^{-\epsilon/2} \left\{ \frac{1}{3} + \frac{\epsilon - 10}{120\epsilon} A^2 + O(A^4) \right\}. \quad (17)$$

Besides solution  $A = 0$ , we have  $A \sim \pm\mu^{1/2}$  (where  $\mu \equiv Pe - Pe_1 = Pe - 3e^{\epsilon/2}$ ), which is a classical pitchfork bifurcation. We thus observe that introducing consumption regularizes the singular bifurcation. More precisely, two conditions are satisfied: (1) the solutions of the regularized equation (17) tend to the solutions of the singular equation (13) for  $\epsilon \rightarrow 0$  and (2) the equation (17) for any  $\epsilon > 0$  has a regular expansion around  $A = 0$ , so that the solutions of this equation undergo a regular pitchfork bifurcation. Similarly, setting the concentration field to zero at a finite distance from the particle center provides a different regularization of Eq. (13). The inverse domain size serves as the regularization parameter in this case.

Based on the analysis of the simplified model presented above, we argue that a similar regularization occurs in the full model of an autophoretic particle in an infinite domain. Namely, the bifurcation is singular for an exact solution of the full problem in an infinite domain but is regularized in a finite domain. The finite domain can be obtained by setting the concentration to zero at a given distance from the particle as a boundary condition. This is often done in analytical or numerical simulations in two dimensions to avoid logarithmic divergence of the concentration field with the distance from the particle. Regularization can also appear in numerical solutions due to discretization of the spatial fluid domain, which effectively sets the finite size of the system. This explains the contradiction between the findings reported in analytical [10–12] and numerical [16] studies.

#### IV. REGULARIZATION THEORY

Exactly solvable problems are an oddity in nonlinear sciences. In the absence of an exact solution, perturbative expansions are often used. Singular bifurcations considered in this work cannot be obtained from a regular perturbative expansion. Although singular perturbative expansions can be obtained directly, for example using the boundary-layer methods [10,11], it may be tempting to use the perturbative

expansion of the regularized problem to analyze the singular limit. The feasibility of the latter approach is analyzed in this section.

In its general form, the regularized pitchfork bifurcation is written as

$$AF(A, \mu, \epsilon) = 0, \quad (18)$$

where  $\mu$  is the parameter measuring distance from the bifurcation point,  $\epsilon \geq 0$  is the regularization parameter, and  $A$  is the perturbation amplitude, such that  $A = 0$  corresponds to the high symmetry solution. The  $A = 0$  solution is often simple enough to be obtained explicitly. For example, this solution corresponds to a stationary autophoretic particle in the problem considered above. The defining property of the pitchfork bifurcation is that the function  $F$  is invariant under the change of sign of  $A$ , which must follow from the symmetry of the underlying physical problem. As above,  $\mu = 0$  is the critical point for which the  $A = 0$  solution loses stability. The function  $F$  is analytic in  $A$  in some interval around  $A = 0$  for  $\epsilon > 0$ . As such, it can be approximated for small-enough  $|A|$  by a Taylor series of form

$$F(A, \mu, \epsilon) = \sum_{k=0}^{\infty} a_k(\mu, \epsilon) A^{2k}, \quad (19)$$

where the coefficients  $a_k(\mu, \epsilon)$  can be calculated using standard perturbation approaches. In practice, only the first several terms of the expansion (19) can be computed for most problems, since the complexity of symbolic calculation of  $a_k$  grows very quickly with  $k$ .

We further consider that there is a well-defined singular limit for  $\epsilon \rightarrow 0$  of the regularized problem,

$$F(A, \mu) \equiv \lim_{\epsilon \rightarrow 0} F(A, \mu, \epsilon), \quad (20)$$

such that the function  $F(A, \mu)$  has a singularity at  $A = 0$ . The general question considered in this section is to which extent the properties of the singular problem defined by the function  $F(A, \mu)$  can be deduced from the first several terms of the expansion (19) of the regularized problem. We first consider the function  $F$  defined by Eqs. (13) and (16), derived in the previous section and then discuss the general case.

The truncated series (17) is what one would have obtained by an analytical expansion in  $A$  in the absence of the exact solution. By trying to compare it (dashed lines in Fig. 3, right panel) to the exact solution [(16), solid lines in Fig. 3, right] in the vicinity of bifurcation where  $A$  is small one realizes that for given  $\mu$  the smaller  $\epsilon$  is the worse the approximation (17) is, and *a fortiori* this expression can in no way account for the singular limit  $\epsilon = 0$ , a limit where the coefficients of the series (17) diverge. This problem cannot be solved simply by including more orders in the perturbative expansion of Eq. (16), as shown in Fig. 3, left panel.

The crux of our theory is the observation that the singular behavior in the above model is due to the existence of a singular point (branch point in this case) in the complex plane, namely  $A = \pm i\epsilon$ , arising from  $\sqrt{A^2 + \epsilon^2}$  in (16). Since Eq. (18) is always satisfied by the trivial solution  $A = 0$ , we focus on the behavior of  $F(A, \mu, \epsilon)$ . The singularity in the complex plane limits the radius of convergence of the expansion (19) to  $|A| < \epsilon$ . For  $|A| > \epsilon$ , the series (19) diverges and



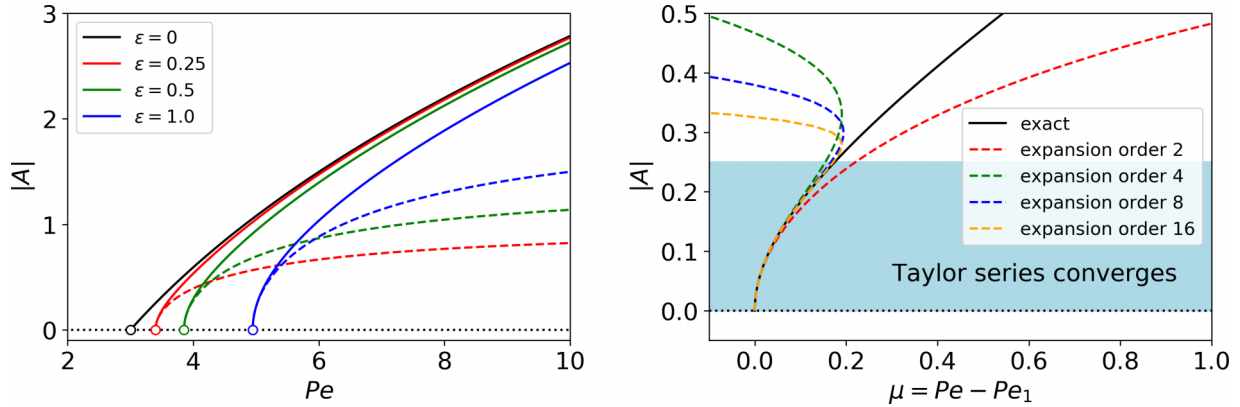


FIG. 3. Convergence of the Taylor series for regularized bifurcations. Left: Leading-order approximation for several values of the regularization parameter  $\epsilon$ . Solid lines: Exact result (16). Dashed lines represent classically expanded solution Eq. (17). Right: The effect of including higher-order terms in the Taylor series of Eq. (16). Shaded area marks the region of convergence of the Taylor series, in which including higher-order terms improves the precision of the expansion.  $\epsilon = 0.25$ ,  $Pe_1 = 3e^{\epsilon/2} \approx 3.40$ .

thus does not provide a good approximation for  $F$  no matter how many terms are taken into account. We therefore arrive at two mutually exclusive conditions on  $\epsilon$  for approximating the singular limit for given  $A$  and  $\mu$ : On the one hand,  $\epsilon$  needs to be sufficiently small to approximate the singular limit, and, on the other hand, it has to be large enough for the series (19) to converge. As Fig. 3 shows, these two conditions cannot be satisfied at the same time.

One could then be tempted to say that (17) is of little practical interest for  $\epsilon$  close to zero. However, and this is the main point, we will be able, in a way that may seem a little surprising, to extract from analysis of a regular expansion (17) the singular behavior  $|A| \sim \mu$  (for  $\epsilon \rightarrow 0$ ) dictated by the exact calculation (16), without any *a priori* knowledge on the exact solution. Moreover, we will regularize the expression (17) in such a way that it represents correctly the exact behavior when  $\epsilon$  is nonzero but small.

To this end, we introduce a change of variables and match expansion coefficients to obtain a series with larger region of convergence. Namely, we propose the following transformation:

$$\epsilon = |A_0|(1-s), \quad A^2 = A_0^2(2s-s^2) \quad (21)$$

with  $A_0$  a real number (recall that  $\epsilon$  is positive). Thanks to this transformation  $A^2 + \epsilon^2 = A_0^2$  remains constant.  $s$  is a parametrization, and the singular limit corresponds to  $s = 1$ . The above transformation means that instead of taking the singular limit  $\epsilon \rightarrow 0$  at given  $A$ , we move in the plane  $(A, \epsilon)$  along the circle of radius  $A_0$ . This transformation renders the expansion in terms of  $s$  regular since  $A^2 + \epsilon^2$  is constant along the circle. Another way to appreciate our choice is that the singularity in the original coordinate,  $A^2 = -\epsilon^2$ , reads  $A_0^2(1-(s-1)^2) = -A_0^2(1-s)^2$ , and which has no solution meaning that in terms of  $s$  variable the original singularity has been moved to infinity. This guarantees absolute convergence of series in term of  $s$ . The procedure consists now in substituting in the expansion (19), truncated at the highest available order,  $A$  and  $\epsilon$  as functions of  $s$  and  $A_0$  [Eq. (21)] and expanding the result in a Taylor series in terms

of  $s$  as

$$\begin{aligned} \tilde{F}(s, A_0, \mu) &\equiv F[A(A_0, s), \mu, \epsilon(A_0, s)] \\ &= \sum_{k=0}^{\infty} a_k[\mu, A_0(1-s)](2s-s^2)^{2k} A_0^{2k} \\ &= \sum_k b_k(\mu, A_0) s^k. \end{aligned} \quad (22)$$

The relation between  $b_k$  and  $a_k$  is easily deduced (see Appendix C). An important observation is that the coefficient  $b_k$  depends only on coefficients  $a_{k'}$  with  $k' \leq k$ . It is therefore possible to calculate the first terms in the  $s$  expansion of  $\tilde{F}$  from a truncated  $A$  expansion of  $F$ . Close to the bifurcation point  $A_0$  is small, so we will retain only  $b_0$ ,  $b_1$ , and  $b_2$ . Let us illustrate the study on the autophoretic system. Taylor expansion of (16) to order  $A^4$  [in the form (19)] yields

$$\begin{aligned} a_0(\epsilon) &= Pe \frac{e^{-\epsilon/2}}{3} - 1, \quad a_1(\epsilon) = Pe \frac{1-10/\epsilon}{120} e^{-\epsilon/2}, \\ a_2(\epsilon) &= Pe \frac{\epsilon^3 - 28\epsilon^2 + 140\epsilon + 280}{13440\epsilon^3} e^{-\epsilon/2}. \end{aligned} \quad (23)$$

from which the coefficients  $b_0$ ,  $b_1$ , and  $b_2$  are determined as

$$\begin{aligned} b_0 &= Pe \frac{e^{-|A_0|/2}}{3} - 1, \quad b_1 = Pe \frac{e^{-|A_0|/2}}{60} A_0^2 \\ b_2 &= Pe \frac{e^{-|A_0|/2}}{3360} A_0^4 - Pe \frac{e^{-|A_0|/2}}{120} A_0^2. \end{aligned} \quad (24)$$

The singular limit is approximated by evaluating the truncated  $s$  series of  $\tilde{F}(s, A_0, \mu)$  at  $s = 1$ , which corresponds to  $\epsilon = 0$ . The first three terms, with coefficients given in Eqs. (24) expanded in powers of  $A_0$ , yield [using  $F(A_0, \mu) \equiv F(A_0, \mu, 0) = \tilde{F}(s=1, A_0, \mu) \approx b_0 + b_1 + b_2$ ]

$$F(A_0, \mu) = Pe[1/3 - |A_0|/6 + |A_0|^2/20 + O(|A_0|^3)] - 1. \quad (25)$$

A remarkable feature is that due to our regularization theory we are able to extract, by using the traditional analytical expansion (19) of the regularized problem, the singular behavior

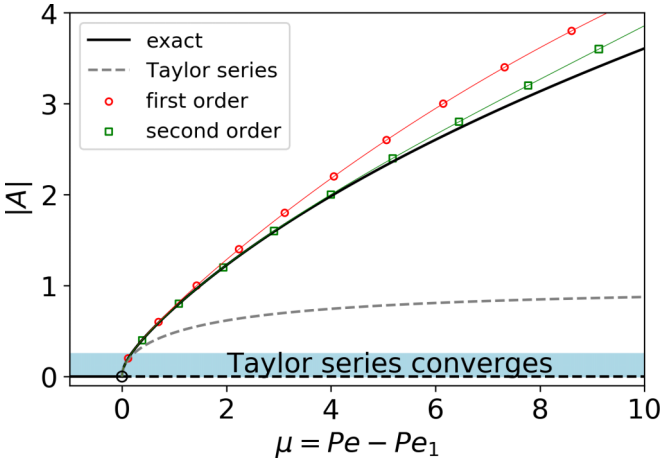


FIG. 4. Reconstructing the regularized bifurcation from its Taylor series. Solid line: Exact result (16). Dotted line represents classically expanded solution Eq. (17). Circles represent the first-order regularized solution Eq. (26). These circles almost coincide with solid lines (exact solution), despite that only leading order in Eq. (26) is retained. Squares represent second-order regularized solution, which provides an even better approximation. Shaded area represents the region of convergence of the Taylor series of the regularized solution at  $A = 0$ ,  $\epsilon = 0.25$ ,  $Pe_1 = 3e^{\epsilon/2} \approx 3.40$ .

exhibiting the absolute value  $|A|$ . Referring to the exact result obtained in the limit  $\epsilon = 0$  [Eq. (13)], we can check that to leading order in  $A$  we obtain exactly the result (25) (recall that we omit the trivial solution  $A = 0$ ). This shows the consistency of the theory.

Another virtue of the theory is that it allows us to transform the expansion (17), which has a small radius of convergence of order  $\epsilon$ , into a form having a wider radius of convergence by applying the method above (used for  $\epsilon \rightarrow 0$ ) for a finite  $\epsilon$  with a corresponding value  $A$ . For that purpose we use the substitutions  $A_0 = \sqrt{A^2 + \epsilon^2}$  and  $s = 1 - \epsilon/\sqrt{A^2 + \epsilon^2}$  in the second expression of (22). To leading order in  $s$  we get  $F(A, \mu, \epsilon) = b_0 + b_1s + O(s^2)$ . As an illustration for the phoretic model the function  $F$  takes now the form (to leading order)

$$F(A, \mu, \epsilon) \approx \mu \frac{e^{-\sqrt{A^2 + \epsilon^2}/2}}{3} \left[ 1 + \frac{A^2 + \epsilon^2}{20} - \frac{\epsilon \sqrt{A^2 + \epsilon^2}}{20} \right] - 1 \quad (26)$$

instead of (17). Note that this expression was obtained using only the first two terms of the expansion of the regularized problem into powers of  $A$ . Neither the singular limit nor the full regularized expression were required. We are also using implicitly the knowledge that the only singular points of the regularized equation are  $A = \pm i\epsilon$  but we show below that the method works even for the case of multiple purely imaginary singular points, the precise location of which is not known. It can be checked that expression (26) reduces to (17) after expansion in  $A$  to order 2. Figure 4 summarizes the results. Use of expansion (17) (dotted line in Fig. 4) fails to capture properly the bifurcation obtained from the exact result (Eq. (16), represented by solid line in Fig. 4). In contrast

(26)—circles in Fig. 4—impressively captures the exact result [Eq. (16), solid lines in Fig. 4]. Even better agreement with the exact result is obtained by taking the expansion (26) to the next order (squares in Fig. 4). The regularization theory not only accounts properly for the singular limit [ $\epsilon = 0$ ; Eq. (25)] but also offers a precious way to approach this limit [Eq. (26)].

## V. GENERALIZATION TO ARBITRARY LOCATION OF SINGULARITIES

### A. General considerations

In the example above the singular points of the regularized problem were located at  $A = \pm i\epsilon$ . This knowledge was used implicitly to construct the transformation that allows us to extract the singular limit from several leading terms of the Taylor series of the regularized problem. In practical applications, the location of the singularities in the complex plane is not known *a priori*. It is therefore necessary to check under what conditions the proposed transformation can be applied. This task is *a priori* nontrivial, and we will see how this question can be tackled in our spirit.

The function  $F$  in Eq. (18) is an analytic function of  $A$  with exception of singular points  $A_i(\epsilon) = \Delta_i\epsilon$ . Here we allow  $\Delta_i$  to be arbitrary complex numbers. Applying the transformation  $\epsilon = A_0(1 - s)$  and  $A^2 = (2s - s^2)A_0^2$  [Eq. (21)], we obtain a function  $\tilde{F}$  of  $s$  and  $A_0$  [as written in the first line of Eq. (22)]. This function is an analytical function of  $s$  with exception of singular points  $s_i$  given by

$$s_i = 1 \pm \frac{1}{\sqrt{1 + \Delta_i^2}}. \quad (27)$$

The radius of convergence of the expansion of  $\tilde{F}$  in powers of  $s$  in Eq. (22) is governed by the singular point  $s_i$  with the lowest absolute value. The success of the proposed method requires this radius of convergence to be at least 1. The method thus works if all  $\Delta_i$  are such that  $|s_i| > 1$ , where  $s_i$  is given by (27). Figure 5 shows the region of the complex plane which must contain  $\Delta_i$  for all singular points of  $\tilde{F}$  in order for the expansion in  $s$  to converge for  $s = 1$ .

### B. Multiple singularities on the imaginary axis

Here we show how the singular function  $F(A, \mu)$  can be recovered from the perturbative expansion of the regularized function  $F(A, \mu, \epsilon)$ , even if the function  $F(A, \mu, \epsilon)$  has multiple singularities on the imaginary axis. Among all singularities of  $F$ , we take the one with the smallest absolute value for given  $\epsilon$ , which determines the radius of convergence of the  $A$  series of  $F$ . We write this singularity as  $A = \pm \Delta_0\epsilon$ . Applying the transformation

$$\epsilon = A_0(1 - s)/\Delta, \quad A^2 = (2s - s^2)A_0^2 \quad (28)$$

with  $\Delta = |\Delta_0|$  for given  $A_0$  and  $\mu$  reduces the function  $F(A^2, \mu, \epsilon)$  to a function of  $s$ . The singularities of this function of  $F$  are given by

$$s_i = 1 \pm \frac{\Delta}{\sqrt{\Delta^2 + \Delta_i^2}}, \quad (29)$$

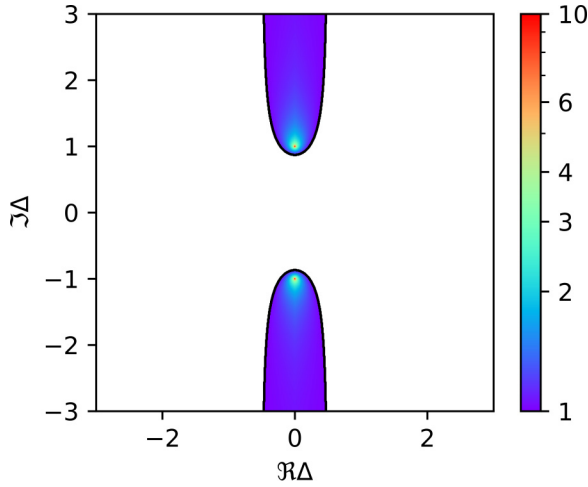


FIG. 5. The radius of convergence of the expansion of  $\tilde{F}$  in powers of  $s$  (22) as a function of the proportionality coefficients  $\Delta_i$  setting the singular points of  $\tilde{F}$  as a function of  $\epsilon$ . The black curves mark the boundary of the region of  $\Delta$  for which the radius of convergence is greater than 1. Only this region is colored.

where  $\Delta_i$  are complex numbers such that the set  $\Delta_i \epsilon$  defines the singularities of the function  $F(x, \mu, \epsilon)$  for a given  $\epsilon$ . Here all numbers  $\Delta_i$  are on the imaginary axis and we have  $|\Delta_i| \geq |\Delta_0|$ . This implies that all singular points in the  $s$  domain lie on a line  $\text{Re}s_i = 1$ . The expansion (22) of  $\tilde{F}$  in powers of  $s$  thus has the radius of convergence of at least one. If the set of singularities  $\Delta_i \epsilon$  is infinite with the absolute values  $|\Delta_i|$  increasing to infinity, then the singular points  $s_i$  given by Eq. (29) have an accumulation point at  $s = 1$ . This implies an essential singularity at  $s = 1$  and the radius of convergence of the expansion (22) of  $\tilde{F}$  in powers of  $s$  being exactly 1. We show that this still allows us to reconstruct the limit of  $s \rightarrow 1$ . Indeed, for any  $s < 1$  the expansion (22) of  $\tilde{F}$  in powers of  $s$  converges and thus taking a sufficient number of terms in the  $s$  expansion of  $\tilde{F}$  would allow us to approximate  $\tilde{F}$  correctly. Since the limit of  $F(A, \mu, \epsilon)$  for  $\epsilon \rightarrow 0^+$  is well defined, so is the limit of  $\tilde{F}$  for  $s \rightarrow 1^-$ . For a given number of known terms in the  $s$  expansion of  $\tilde{F}$ , the approximation error of  $\tilde{F}$  at  $s = 1$  and a given value of  $A_0$  is a combination of two contributions: the difference of exact values of  $F(A(s, A_0), \mu, \epsilon(s, A_0)) - F(A(1, A_0), \mu, \epsilon(1, A_0)) \equiv F(A(s, A_0), \mu, \epsilon(s, A_0)) - F(A_0, \mu)$  and the difference of the exact value  $F(A(s, A_0), \mu, \epsilon(s, A_0))$  and its approximation by a truncated series in powers of  $s$ . The first of these contributions decreases as  $s$  approaches 1, while the second one in general decreases as  $s$  is decreased. There is thus a compromise of choosing the correct value of  $s$  to approximate  $F(A_0, 0)$  as the sum of the truncated  $s$  series of  $F(A(s, A_0), \mu, \epsilon(s, A_0))$ . We can argue, however, that including more terms in the truncated series leads to a higher optimal value of  $s$  and thus better precision of the overall approximation.

### C. Example of multiple singularities on the imaginary axis

As a practical example of this method, we consider the expression of particle velocity in a finite-size domain, given

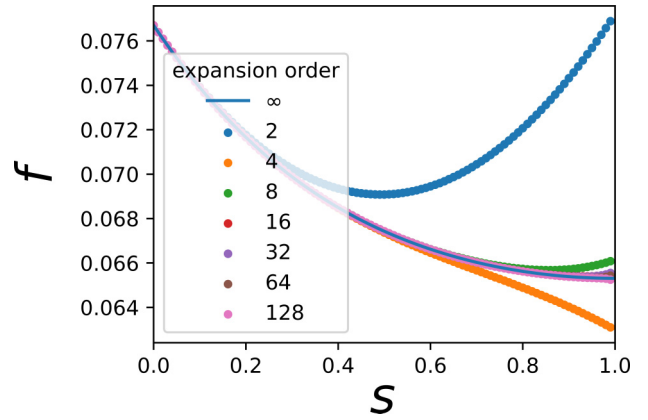


FIG. 6. Function  $F$  defined by (16) with change of variables  $F(A(s, A_0), \mu, \epsilon(s, A_0))$  shown as a function of  $s$  (solid line). Symbols show the approximation of  $\tilde{F}$  using the truncated series of  $F$  for several truncation orders.

by Eq. (B9) in Appendix B. The singularities of this equation correspond to simple poles given by the solutions of  $\sinh A/(2\epsilon) = 0$  with  $A \neq 0$ . There is also an essential singularity at infinity. The poles of  $F$  thus lie on the imaginary axis and correspond to  $A = \pm 2\pi i \epsilon k$  with positive integer  $k$ . The region of convergence of the Taylor series is thus given by  $|A| < 2\pi\epsilon$ . Performing the change of variables (28) with  $\Delta = 2\pi$ , we rewrite the function  $F$  as a series in powers of  $s$ :

$$\tilde{F}(s, A_0, \mu) \equiv F(x(s, A_0), \mu, \epsilon(s, A_0)) = \sum_{k=0}^{\infty} b_k(A_0, \mu) s^k, \quad (30)$$

where a coefficient  $b_k(A_0)$  can be explicitly computed through coefficients  $a_{k'}$  with  $k' \leq k$  in the expansion (19) and their derivatives, as given in Eqs. (C2) for the leading terms. We also tried different values of  $\Delta$  in Eq. (28) and confirmed that the method still converges to the correct result, although a higher number of terms might be needed compared to  $\Delta = 2\pi$  to achieve the same precision. This shows that the exact expression of the radius of convergence of the Taylor series as function of  $\epsilon$  is not necessary to apply the proposed method. It is sufficient to get an estimate of the convergence radius from the coefficients  $a_k(\epsilon)$  by a conventional method, such as computing the sequence  $|a_k(\epsilon)|^{1/k}$  for a given  $\epsilon$ . The only condition that needs to be satisfied is that the smallest absolute value of the singular points in the  $s$  domain defined by Eq. (29) be at least one. This implies that we can overestimate the radius of convergence of the Taylor series (19) by a factor of  $2/\sqrt{3}$  and still get a convergent series in  $s$ .

The results are presented in Figs. 6 and 7. First, we plot the exact expression of  $\tilde{F}$  as a function of  $s$  and its approximation by a truncated series for several orders of truncation (Fig. 6). We observe that indeed increasing the number of terms in the truncated series allows to expand the region of its applicability as close to 1 as necessary.

Second, we show how the truncated series of  $\tilde{F}$  converges to the exact value as the number of terms is increased for a given  $s$  (Fig. 7). It is seen that convergence is faster for smaller values of  $s$ . This shows that indeed the correct value of  $f$

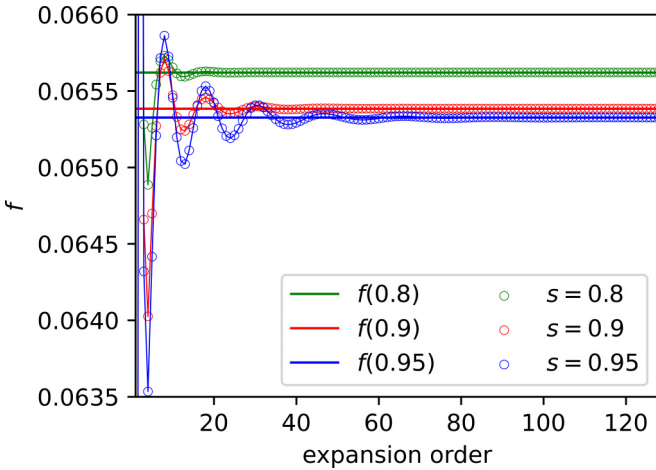


FIG. 7. Convergence of the truncated series (30) to the exact value as a function of the number of terms for several values of  $s$  (symbols). Solid lines show the exact values.

for  $s = 1$  (or, equivalently,  $\epsilon = 0$ ) can be extrapolated from expansion (19) by computing the truncated series (30) for  $s$  close to 1. The optimal value of  $s$  depends on the number of terms taken in expansion (30) and approaches 1 as the number of terms is increased.

Finally, we show the full bifurcation diagram of Eq. (B9) reconstructed from the truncated Taylor series (19) using the transformation (28). We consider both the singular limit  $\epsilon = 0$  and the regularized problem ( $\epsilon = 0.05$ ) (Figs. 8, left and right, respectively). As evident from this figure, the singular behavior close to the bifurcation point can be recovered only using the first terms of the series (19). Taking further terms in expansion (30) increases the precision of the approximation and allows us to recover the correct bifurcation diagram far from the bifurcation point.

### VI. CLASSIFICATION OF SINGULAR BIFURCATIONS

The singular bifurcations discussed above are related to a branch point of the complex square root. In general, more

complicated singular bifurcations can be constructed. Let us briefly consider different options on the basis of the behavior of the function  $F$  in (18). Suppose that the singularity is due to the presence of terms of the form  $(A^2 + \epsilon^2)^\alpha$ , where  $\alpha$  is real noninteger positive number such that  $\alpha < 1$ . Following the general procedure presented above, we straightforwardly obtain to leading order the singular limit,

$$F(A, \mu) = \mu - |A|^{2\alpha}, \tag{31}$$

where we have rescaled  $A$  so that the coefficient in front of the singular term can be set to unity. Note that if we took  $\alpha > 1$ , then the first dominant term is  $A^2$  and to leading order the expansion would be regular. We assume here a supercritical bifurcation, and this is why we set the coefficient of the first nonlinear term to be negative. In terms of a dynamical system, and by remembering that we assume  $A = 0$  to exist always as a solution, the corresponding normal form is

$$\dot{A} = \mu A - A|A|^{2\alpha}. \tag{32}$$

Equation (32) constitutes the generic normal form of an algebraic singular bifurcation. The nontrivial fixed point behaves as  $A \sim \pm \mu^{1/(2\alpha)}$ . The bifurcation structure is qualitatively different depending on whether  $\alpha > 1/2$  or  $\alpha < 1/2$ . In the first case the bifurcation diagram is similar to a pitchfork bifurcation with infinite slope at  $\mu = 0$ , whereas in the second case the slope vanishes for  $\mu = 0$ .  $\alpha = 1/2$  is a special case with finite slope. Finally, for  $\alpha < 0$  the normal form is

$$\dot{A} = \mu A + A|A|^{2\alpha}. \tag{33}$$

We adopted the positive sign in front of the nonlinear term to guarantee a stable branch for  $A \neq 0$ . Note that this does not affect the bifurcation diagram topology. The nontrivial fixed point is given  $A \sim \pm(-\mu)^{1/(2\alpha)}$ . Figure 9 summarizes the results. We note four different singular bifurcations (in blue in Fig. 9) corresponding to (i)  $\alpha > 1/2$ , (ii)  $\alpha < 1/2$ , (iii)  $\alpha = 1/2$ , and (iv)  $\alpha < 0$ . We refer to these four singular bifurcations as (i) fold, (ii) cusp, (iii) angular, and (iv) unbounded. When these bifurcations are regularized, they all fall into a pitchfork bifurcation (Fig. 9). We may refer to the above

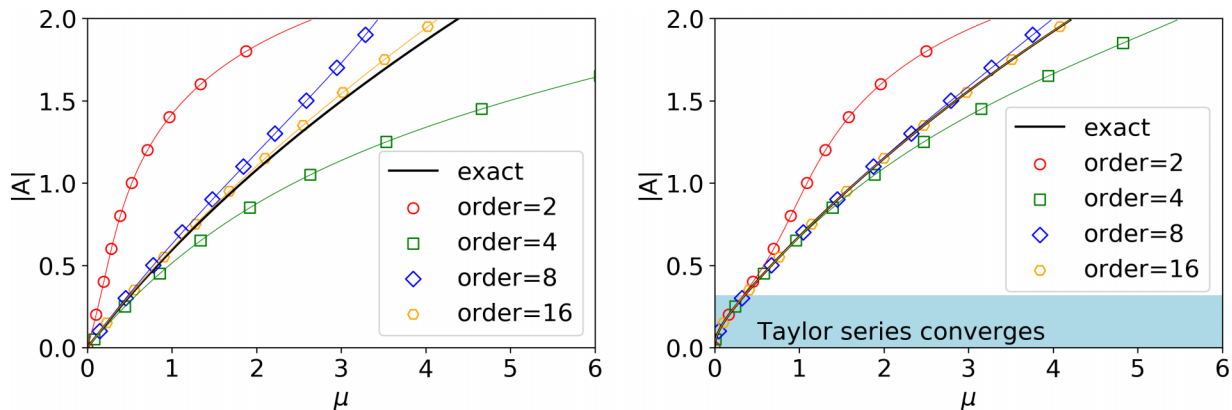


FIG. 8. Bifurcation diagrams for regularized problem with multiple singularities on the imaginary axis. See Eq. (B9) for the explicit form of the equation. Comparison between the truncated  $s$  series (30) and the exact result for several orders of the expansion. Left: Singular problem ( $\epsilon = 0$ ). Right: Regularized problem with  $\epsilon = 1/20$ . The shaded area marks the region of convergence of the original Taylor series (19)  $|A| < 2\pi\epsilon \simeq 0.314$ .



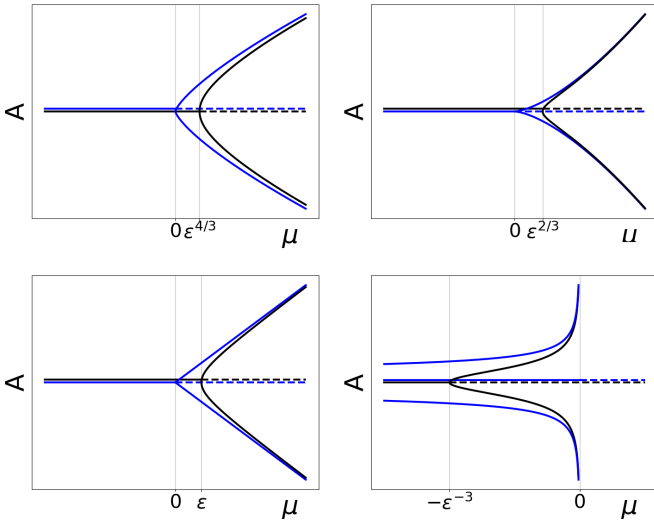


FIG. 9. Diagram for the four different singular bifurcations (in blue) and for their regularized form (in black), with  $\alpha = 2/3$ ,  $\alpha = 1/3$ ,  $\alpha = 1/2$ , and  $\alpha = -3/2$ . Solid lines refer to stable solutions and dashed lines to unstable ones.

bifurcations as *singular pitchfork bifurcations* as well, albeit the singular limits have different behaviors.

It must be noted that the above classification does not exhaust by far all kinds of singularities. For example, the 2D phoretic model provides an example of transcendental singularity where the velocity behaves as  $\tilde{V}_0 \sim e^{-2/P\epsilon}$  (see Appendix D). Finally, the classification can easily be generalized to other bifurcations, which degenerate into other bifurcations than the pitchfork one (e.g., saddle-node and subcritical bifurcations) after regularization.

The exponent  $\alpha$  can be related to the Taylor expansion (19) of the regularized problem in a straightforward way: Close to the critical point, Eq. (19) can be transformed to a canonical form,

$$\mu - \sum_{k=0}^{\infty} \tilde{a}_k(\epsilon) A^{2k} = 0, \quad (34)$$

by neglecting the terms of order  $O(\mu^2)$  and dividing Eq. (18) by the coefficient in front of  $\mu$ . Here  $\tilde{a}_k(\epsilon)$  are coefficients related to the coefficients of the original series (19). Consider now that the coefficients  $a_k$  scale as  $a_k(\epsilon) \sim \epsilon^{p-2kq}$  for  $\epsilon \rightarrow 0$ . From this, we first conclude that the radius of convergence of the series in Eq. (34) scales as  $\epsilon^q$ . Using the radius of convergence as the new regularization parameter  $\tilde{\epsilon}$ , we get  $a_k(\tilde{\epsilon}) \sim \tilde{\epsilon}^{p/q-2k}$ . Applying the transformation (21) with  $\epsilon$  replaced by  $\tilde{\epsilon}$  and truncating the series to the zeroth order in  $s$ , we obtain an expression of form (31) with  $\alpha = p/(2q)$ .

## VII. CONCLUSION

This study has brought to light a problem that has gone unnoticed in the field of nonlinear science, in spite of its old age of foundation. A singular behavior was encountered in the early 1990s for moving drops [10] but was not highlighted. We have seen here that the dogma of a regular expansion in bifurcation theory has its limits, which can lead to meaningless

results. The absence of exact analytical results in nonlinear systems has not allowed to draw easily attention to the singular character of bifurcations.

We have provided a framework to deal with singular bifurcations. The few concrete examples mentioned in the Introduction are far from having exhausted all cases where singular bifurcations manifest themselves. Several numerical studies could have alerted to the nonstandard character of bifurcations. For example, Sauzade *et al.* [26] analyzed the speed of the Taylor swimmer sheet in perturbation theory as a function amplitude of the swimmer deformation by including up to 1000 terms in the series expansion. They found that the series diverges beyond an amplitude of deformation. This is symptomatic of a hidden singularity in the model. In another problem, that of vesicles (a simple model of red blood cells) in a flow [27,28], the perturbative scheme for vesicle dynamics (in power series of excess area from a sphere) has a small range of applicability even when including higher and higher-order terms in the series expansion. This is indicative of potential singularity in complex plane. It is hoped that this study serves as a general framework to analyze singular bifurcations for explicit nonlinear models.

The topic of this work is the regularization of singular bifurcations. The bifurcation diagram is thus defined by solutions of an equation that is singular for order parameter equal to 0. It is also possible for solutions of a regular bifurcation problem to have singular expansions [29,30], in what is called an imperfect bifurcation, when a small perturbation of the equation changes qualitatively the bifurcation diagram. We note, however, that the problem considered in this work is completely different because for imperfect bifurcations, the equation that defines the problem can be well approximated by a truncated power expansion in  $A$ ,  $\mu$ , and  $\epsilon$  (as considered in Ref. [29]), from which the singular limit  $\epsilon = 0$  follows automatically. The singularities for imperfect bifurcations appear only in solutions of the equation defining the problem.

The example of phoretic particle considered in this work corresponds to  $\alpha = 1/2$  in 3D (order parameter grows linearly above the critical point) and to  $\alpha = 0$  in 2D (order parameter grows as  $e^{-1/\mu}$  for  $\mu > 0$ ; see an explicit example in Appendix D). An interesting question is whether other values of  $\alpha$  can be encountered in physical problems. Phase transitions in thermodynamics can be characterized by fractional or irrational critical exponents (e.g.,  $1/8$  for magnetization in 2D Ising model [31]). They are also known to be regularized by finite system size. Similarly to the problems considered in this work, the critical points for thermodynamic phase transitions correspond to singularities of the thermodynamic potentials (zeros of the partition function). These singularities are located in the complex plane of inverse temperature for finite systems but tend to the real axis in the thermodynamic limit. Despite these similarities, the modeling of the phase transitions in thermodynamics is quite different from the problems considered here, which prevents us from drawing a more direct analogy.

The singular behavior appears for autophoretic particles due to the divergence of the characteristic length scale of the concentration field close to the critical point. This dependence of the length scale on the distance from the critical point can be related to the distribution of the eigenvalues of the linear

stability operator of the stationary solution. This suggests that the spectrum of the linear stability operator of the unperturbed solution can be related to the exponent  $\alpha$  of the singular bifurcation. Analyzing this relationship can be an interesting question for further research.

The absolute value function, which appears in the singular limit of the problem considered in this study, can be viewed as a generic piecewise smooth function. The dynamic systems defined by discontinuous functions are a topic of active research (as shown in a recent review [32]). Such systems can show bifurcations not observed for classical systems. Regularization is an important tool used in studies of discontinuous multidimensional systems to link the bifurcation type in the discontinuous limit to the behavior of the regularized system (as reviewed in Ref. [33]). In contrast to the present study, the regularization in these works was applied in a finite vicinity of the discontinuity only and the regularized function was still not analytical at the boundary of the regularization region.

### ACKNOWLEDGMENTS

We thank S. Michelin for stimulating discussions. We thank Centre National d'Etudes Spatiales for financial support and for having access to data of microgravity, and the Franco-German University programme "Living Fluids" (Grant CFDA-Q1-14) for financial support.

### APPENDIX A: EFFECT OF HYDRODYNAMICS ON CRITICAL CONDITION

The goal of this section is to introduce the corrections into the exactly solvable model in order to account for the finite size of the particle. These corrections are evaluated for small propulsion velocity and provide quantitatively correct value of the critical Peclet number. There are two finite-size effects that are neglected in the main model: First, the near-field flow disturbance due to a translating spherical particle is neglected and, second, the particle emission is represented by a point source, while the finite-size particle should be represented by a distribution of sources along the particle surface. Both of these two effects are essential for quantitative evaluation of the concentration field close to the critical point.

This problem is solved in the reference frame comoving with the particle. The concentration evolution equation is then written as

$$\dot{c}(\mathbf{r}) + \nabla \cdot (\mathbf{u}(\mathbf{r})c(\mathbf{r})) = D\nabla^2 c(\mathbf{r}) + S(\mathbf{r}), \quad (\text{A1})$$

where  $\mathbf{u}(\mathbf{r})$  is the fluid velocity relative to the particle,  $S(\mathbf{r})$  represents a distribution of sources and source dipoles on the particle surface which accounts for the concentration emission or consumption, and  $\mathbf{r}$  is the position vector relative to the particle center. It is known that the velocity field in the comoving frame can be written as

$$\mathbf{u}(\mathbf{r}) = -\mathbf{V}_0 + \frac{a^3}{2r^3} \left[ 3 \frac{\mathbf{r}(\mathbf{r} \cdot \mathbf{V}_0)}{r^2} - \mathbf{V}_0 \right] \quad (\text{A2})$$

for a rigid force-free spherical particle of radius  $a$ , moving with velocity  $\mathbf{V}_0$  relative to the laboratory frame. The flow field in Eq. (A2) can be written in potential representation

$\mathbf{u}(\mathbf{r}) = \nabla\phi(\mathbf{r})$ , where

$$\phi(\mathbf{r}) = -(\mathbf{V}_0 \cdot \mathbf{r}) \left( 1 + \frac{a^3}{2r^3} \right). \quad (\text{A3})$$

We also have  $\nabla^2\phi(\mathbf{r}) = 0$  for  $r > 0$  due to the flow incompressibility.

We focus on the steady-state solution of Eq. (A1). Multiplying Eq. (A1) by  $\exp[-\phi(\mathbf{r})/(2D)]$ , yields

$$D\nabla^2 \bar{c}(\mathbf{r}) - \frac{u(\mathbf{r})^2}{4D} \bar{c}(\mathbf{r}) + \bar{S}(\mathbf{r}) = 0, \quad (\text{A4})$$

where  $\bar{c}(\mathbf{r}) = c(\mathbf{r}) \exp[-\phi(\mathbf{r})/(2D)]$  and  $\bar{S}(\mathbf{r}) = S(\mathbf{r}) \exp[-\phi(\mathbf{r})/(2D)]$ .

The original model corresponds to setting  $u(\mathbf{r})^2$  to  $V_0^2$ ,  $\phi(\mathbf{r})$  to  $-\mathbf{V}_0 \cdot \mathbf{r}$ , and  $\bar{S}(\mathbf{r})$  to a point source in Eq. (A4). Here we still simplify  $u(\mathbf{r})^2$  to  $V_0^2$  because this term is quadratic in the particle velocity and thus should be small close to the critical point. We keep, however, the full expression for  $\phi$  and replace the  $\bar{S}(\mathbf{r})$  term with a combination of a point source and a point source dipole. The amplitude of the source dipole is chosen in a way that corresponds to an isotropic emission rate at distance  $a$  from the particle center.

We thus consider the following equation:

$$D\nabla^2 \bar{c}(\mathbf{r}) - \frac{V_0^2}{4D} \bar{c}(\mathbf{r}) + 4\pi a^2 \mathcal{A}[\delta(\mathbf{r}) + b(\mathbf{V}_0 \cdot \nabla)\delta(\mathbf{r})] = 0. \quad (\text{A5})$$

This equation can be solved analytically, yielding

$$\bar{c}(\mathbf{r}) = \frac{a^2 \mathcal{A}}{Dr} \exp\left(-\frac{V_0 r}{2D}\right) + b(\mathbf{V}_0 \cdot \nabla) \left\{ \frac{a^2 \mathcal{A}}{Dr} \exp\left(-\frac{V_0 r}{2D}\right) \right\}, \quad (\text{A6})$$

The constant  $b$  is found by taking the concentration field  $c(\mathbf{r}) \equiv \bar{c}(\mathbf{r}) \exp[\phi(\mathbf{r})/(2D)]$  and setting the first harmonic of  $\mathbf{r} \cdot \nabla c(\mathbf{r})$  to zero:

$$b = \frac{9a^2}{2D} \frac{\xi + 3}{\xi^2 + 6\xi + 18} \frac{(\xi - 2)e^\xi + \xi + 2}{(\xi^2 - 4\xi + 8)e^\xi - (\xi^2 + 4\xi + 8)}, \quad (\text{A7})$$

where  $\xi = 3V_0 a/(2D)$ . Substituting Eq. (A7) into Eq. (A6) yields the corrected concentration field. We extract the first harmonic of the concentration for  $r = a$  from this solution, which gives us the following expression of the swimming velocity:

$$\begin{aligned} V_0 &= -\frac{18\mathcal{A}Ma[(\xi - 2)e^\xi + \xi + 2] \exp(-\frac{5\xi}{6})}{D\xi^2(\xi^2 + 6\xi + 18)} \\ &= -\frac{\mathcal{A}MaV_0}{4D^2} [1 - aV_0/D + O((aV_0/D)^2)]. \end{aligned} \quad (\text{A8})$$

Dividing both sides of Eq. (A8) by  $V_0$  and setting  $V_0$  to 0 yields  $-\mathcal{A}Ma/D^2 \equiv \text{Pe} = 4$  for the critical Peclet number, which agrees with the previous works.

### APPENDIX B: FINITE-SIZE EFFECT

We consider the same phoretic model except that the size is finite. We focus here only on steady-state solutions in the

comoving frame with velocity  $\mathbf{V}_0$ . The concentration field obeys in this frame

$$D\Delta c + \mathbf{V}_0 \cdot \nabla c = -S\delta(\mathbf{r}). \quad (\text{B1})$$

The particle is taken to move along the  $z$  direction. Making the substitution  $c = \bar{c}e^{-\frac{zV_0}{2D}}$  we find

$$\Delta \bar{c} - k^2 \bar{c} = -\frac{S}{D}\delta(\mathbf{r}), \quad k^2 = V_0^2/(4D^2). \quad (\text{B2})$$

This is the so-called screened Poisson equation with a delta source term. The associated Green's function is defined as

$$\Delta G(\mathbf{r}, \mathbf{r}') - k^2 G(\mathbf{r}, \mathbf{r}') = \delta(\mathbf{r} - \mathbf{r}'). \quad (\text{B3})$$

We consider the domain to be finite and bounded by a sphere with radius  $r = R$  (counted from the point source). The boundary condition is taken as  $\bar{c}(r = R) = 0$ . We use the eigenfunctions of the Laplacian in order to express the Green's function. The Laplacian eigenfunctions are spherical harmonics  $Y_\ell^m(\theta, \phi)$  times spherical Bessel functions  $j_\ell(r)$ . Let  $\beta_{\ell n}$  define the zero's of  $j_\ell$ , we have  $j_\ell(\beta_{\ell n}) = 0$ . The Laplacian eigenfunction which vanishes at  $r = R$  can be written as

$$\psi_{n\ell m}(r, \theta, \phi) = A_{n\ell} Y_\ell^m(\theta, \phi) j_\ell(\beta_{\ell n} r/R). \quad (\text{B4})$$

Then making use of the classical method to express the Green's function in terms of eigenfunctions, we obtain

$$G(\mathbf{r}, \mathbf{r}') = -\sum_{n\ell m} \frac{2}{R^3 j_{\ell+1}^2(\beta_{\ell n})} \times \frac{Y_\ell^m(\theta, \phi) j_\ell(\beta_{\ell n} r/R) Y_\ell^m(\theta', \phi') j_\ell(\beta_{\ell n} r'/R)}{k^2 + (\beta_{\ell n}/R)^2}. \quad (\text{B5})$$

Note that the eigenvalues of the Laplacian are  $-(\beta_{\ell n}/R)^2$ , meaning that the eigenvalues of the full operator in (B2) are  $-k^2 - (\beta_{\ell n}/R)^2$ . The above Green's function can be rewritten as

$$G(\mathbf{r}, \mathbf{r}') = -\frac{2}{R^3} \sum_{n\ell} \frac{2\ell+1}{4\pi} P_\ell[\cos(\gamma)] \times \frac{1}{j_{\ell+1}^2(\beta_{\ell n})} \frac{j_\ell(\beta_{\ell n} r/R) j_\ell(\beta_{\ell n} r'/R)}{k^2 + (\beta_{\ell n}/R)^2} \quad (\text{B6})$$

after having used the addition theorem for spherical harmonics, where  $P_\ell$  is the Legendre polynomial of order  $\ell$  and  $\cos(\gamma) = \cos(\theta)\cos(\theta') + \sin(\theta)\sin(\theta')\cos(\phi - \phi')$ . Since the source term is assumed to be at the center, we set  $\mathbf{r}' = 0$ , so that  $j_\ell(\beta_{\ell n} r'/R) = j_\ell(0)$ . Due to the properties of  $j_\ell$  only  $\ell = 0$  survives in the sum. Using the definition of  $j_0$  and  $j_1$  functions, we obtain (on using that  $\beta_{0n} = n\pi$ ) that the concentration field can be written as

$$c(r, \theta) = \frac{A}{4\pi D r} e^{-\frac{rV_0 \cos(\theta)}{2D}} \text{csch}(|k|R) \sinh[|k|(R-r)], \quad (\text{B7})$$

where we have used the result

$$\sum_{n=0}^{\infty} n \sin(na)/(n^2 + b^2) = \pi \text{csch}(\pi|b|) \sinh[(\pi - a)|b|], \quad (\text{B8})$$

$\text{csch}$  being the hyperbolic cosecant function. Projecting  $c(r, \theta)$  on the first spherical harmonic, and using the condition that

$V_0 = -\mathcal{M}c_1/(a\sqrt{3\pi})$  (recall that  $c_1$  is the concentration contribution of the first harmonic at  $r = a$ ), we find

$$A = 4\text{Pe} \left[ \frac{A \cosh(A/2) - 2 \sinh(A/2)}{A^2} \right] \times \frac{\sinh[|A|(1/\epsilon - 1)/2]}{\sinh[|A|/(2\epsilon)]}, \quad (\text{B9})$$

where  $A = aV_0/D$  is the perturbation amplitude and  $\epsilon = a/R$  is the regularization parameter. Expanding this result for small  $A$  we obtain to cubic order

$$A = \frac{\text{Pe}}{3} A \left[ 1 - \epsilon - \frac{A^2}{24} (2\epsilon^{-1} - 3 + \epsilon) \right]. \quad (\text{B10})$$

We see that the expansion is regular; the finite size has regularized the singular pitchfork behavior. The solution  $A = 0$  always exists. Beyond a certain critical value  $\text{Pe} = \text{Pe}_1$  there exists another solution behaving as  $A \sim \pm \mu^{1/2}$ , with  $\mu = \text{Pe} - \text{Pe}_1$  and  $\text{Pe}_1 = 3/(1 - \bar{R}^{-1})$ . The last factor in Eq. (B9) can be transformed as

$$\frac{\sinh[|A|(1/\epsilon - 1)/2]}{\sinh[|A|/(2\epsilon)]} = \cosh(|A|/2) - \coth[|A|/(2\epsilon)] \sinh(|A|/2). \quad (\text{B11})$$

Taking the limit  $\epsilon \rightarrow 0^+$  for fixed  $A \neq 0$  simplifies  $\coth[|A|/(2\epsilon)]$  to 1, transforming Eq. (B11) into  $e^{-|A|/2}$ , which recovers the infinite-size expression (13).

Equation (B9) has an infinite and countable set of singularities on the imaginary axis,  $A = \pm in\pi\epsilon/2$ ,  $n$  being a positive integer. These singularities correspond to the zeros of the function  $\sinh(|A|\epsilon/2)$  in the denominator of (B9).

### APPENDIX C: RELATION BETWEEN $a_k$ AND $b_k$

It is easy to obtain the general relation between  $a_k$  and  $b_k$ . However, here we only list the relations for the first three terms (generalization to arbitrary order is straightforward). The starting point is to write the Taylor expansion in terms of  $a_k(\epsilon)x^{2k}$  and make the substitution  $\epsilon = A_0(1-s)$  and  $A^2 = (2s - s^2)A_0^2$ , so that we have

$$b_0(A_0) + b_1(A_0)s + b_2(A_0)s^2 + \dots = a_0[A_0(1-s)] + a_1[A_0(1-s)](2s - s^2)A_0^2 + a_2[A_0(1-s)](2s - s^2)^2 A_0^4 + \dots \quad (\text{C1})$$

Then expanding  $a_k[A_0(1-s)]$  in Taylor series at  $s = 0$  and matching the coefficients for each power of  $s$ , we obtain to leading order,

$$b_0(A_0) = a_0, \quad b_1(A_0) = -A_0 a_0' + 2a_1 A_0^2, \\ b_2(A_0) = \frac{A_0^2 a_0''}{2} - a_1 A_0^2 - 2A_0^3 a_1' + 4a_2 A_0^4, \quad (\text{C2})$$

where  $a_k$  as well as  $a_k'$  and  $a_k''$ , which designate first and second derivative with respect to  $\epsilon$ , are evaluated at  $\epsilon = A_0$ .

### APPENDIX D: 2D MODEL WITH CONSUMPTION

In 2D we only need to substitute in the denominator of the propagator  $(4\pi\tau)^{3/2}$  by  $4\pi\tau$ , so that the concentration field

takes the form

$$c(\mathbf{r}, t) = \int_0^\infty d\tau \frac{S}{4\pi D\tau} \exp\left\{-\frac{(\mathbf{r} + \mathbf{V}_0\tau - \mathbf{V}_0t)^2}{4D\tau}\right\}, \quad (\text{D1})$$

yielding

$$c(\mathbf{r}, t) = \frac{Aa}{D} K_0\left(\frac{\tilde{r}\sqrt{V_0^2 + 4\beta D}}{2D}\right) e^{-\tilde{r}\tilde{V}_0 \cos(\theta)/(2D)}, \quad (\text{D2})$$

where  $K_0$  is the Bessel function of the second kind. Projecting (B10) on the first Fourier mode and using the equation fixing velocity as a function of concentration (see main text) we find  $V_0 = -\mathcal{M}c_1/a$  (where  $c_1$  is the amplitude of the first Fourier mode), obtaining finally

$$A = 2\text{Pe}I_1(A/2)K_0\left(\frac{\sqrt{A^2 + \epsilon^2}}{2}\right), \quad (\text{D3})$$

where  $I_1$  is the Bessel function of the first kind. Besides the trivial solution, this equation exhibits a motile solution for any value of  $\text{Pe}$ , as shown here.

The right-hand side of (D3) can be expanded for  $\epsilon = 0$  as

$$2\text{Pe}I_1(A/2)K_0(A/2) = -\text{Pe}A[\ln(A/4) + \gamma + O(A^2 \ln A)]/2, \quad (\text{D4})$$

where  $\gamma \simeq 0.577$  is the Euler constant. Here we have used the asymptotic expansions  $I_1(A/2) \simeq A/4$  and  $K_0(A/2) \simeq -\ln(A/4) - \gamma$ . Substituting (D4) into (D3) yields the

following asymptotic solution:

$$A = 4 \exp(-2/\text{Pe} + \gamma). \quad (\text{D5})$$

The Taylor series of the right-hand side of (D3) for finite values of  $\epsilon$  reads

$$F_{2D}(A, \epsilon) = -\text{Pe} \frac{K_0(\epsilon/2)}{2} + \text{Pe} \left[ \frac{K_1(\epsilon/2)}{8\epsilon} - \frac{K_0(\epsilon/2)}{64} \right] A^2 + \text{Pe} \left[ -\frac{K_0(\epsilon/2)}{6144} - \frac{K_0(\epsilon/2)}{128\epsilon^2} + \frac{K_1(\epsilon/2)}{256\epsilon} - \frac{K_1(\epsilon/2)}{32\epsilon^3} - \frac{K_2(\epsilon/2)}{128\epsilon^2} \right] A^4 + O(A^6) - 1, \quad (\text{D6})$$

where  $AF_{2D}(A, \epsilon)$  represents Eq. (D3). The radius of convergence of expansion (D6) is equal to  $\epsilon$ . Using the expressions (C2), we get

$$F_{2D}(A, 0) = -\text{Pe} K_0(A/2)(1/2 + A^2/64 + A^4/1536) - 1, \quad (\text{D7})$$

where we have retained the terms up to  $s^2$  in the expansion of the right-hand side of (D6) in  $s$ . Expansion (D7) agrees with the singular expression (D4) since we have  $2I_1(A/2) = -A/2 - A^3/64 + O(A^5)$ . We have checked that taking more terms in  $s$  and, consistently, truncating the regularized expansion (D6) at a higher power of  $A$  allows us to calculate correctly the higher-order terms in the expansion of  $I_1(A/2)$  in the singular expression (D4).

- 
- [1] D. Stauffer, S. M. M. de Oliveira, P. M. C. de Oliveira, and J. S. de Sa Martins, in *Biology, Sociology, Geology by Computational Physicists*, edited by A. Luo and G. Zaslavsky (Elsevier Science, Amsterdam, 2006).
- [2] S. Fauve, Pattern forming instabilities, in *Hydrodynamics and Nonlinear Instabilities*, edited by C. Godrèche and P. Manneville (Cambridge University Press, 2005).
- [3] D. Goluskin, *Internally Heated Convection and Rayleigh-Benard Convection* (Springer, Berlin, 2015).
- [4] A. M. Turing, *Phil. Trans. R. Soc. Lond. B* **237**, 37 (1952).
- [5] P. Bourgin and A. Lesne, *Morphogenesis Origin of Shape and Patterns* (Springer, Berlin, 2011).
- [6] C. Misbah, *Complex Dynamics and Morphogenesis* (Springer, Berlin, 2017).
- [7] K. Kassner, *Pattern Formation in Diffusion-Limited Crystal Growth: Beyond the Single Dendrite* (World Scientific, Singapore, 1996).
- [8] Y. Saito, *Statistical Physics of Crystal Growth* (World Scientific, Singapore, 1996).
- [9] C. Misbah, O. Pierre-Louis, and Y. Saito, *Rev. Mod. Phys.* **82**, 981 (2010).
- [10] A. Y. Rednikov, Y. S. Ryazantsev, and M. G. Velarde, *Phys. Fluids* **6**, 451 (1994).
- [11] M. Morozov and S. Michelin, *J. Fluid Mech.* **860**, 711 (2019).
- [12] S. Saha, E. Yariv, and O. Schnitzer, *J. Fluid Mech.* **916**, A47 (2021).
- [13] Z. Izri, M. N. van der Linden, S. Michelin, and O. Dauchot, *Phys. Rev. Lett.* **113**, 248302 (2014).
- [14] S. Michelin, E. Lauga, and D. Bartolo, *Phys. Fluids* **25**, 061701 (2013).
- [15] C. Jin, C. Krüger, and C. C. Maass, *Proc. Natl. Acad. Sci. USA* **114**, 5089 (2017).
- [16] W. F. Hu, T. S. Lin, S. Rafai, and C. Misbah, *Phys. Rev. Lett.* **123**, 238004 (2019).
- [17] M. Morozov and S. Michelin, *J. Chem. Phys.* **150**, 044110 (2019).
- [18] A. Izzet, P. G. Moerman, P. Gross, J. Groenewold, A. D. Hollingsworth, J. Bibette, and J. Brujic, *Phys. Rev. X* **10**, 021035 (2020).
- [19] B. V. Hokmabad, R. Dey, M. Jalaal, D. Mohanty, M. Almukambetova, K. A. Baldwin, D. Lohse, and C. C. Maass, *Phys. Rev. X* **11**, 011043 (2021).
- [20] Y. Chen, K. L. Chong, L. Liu, R. Verzicco, and D. Lohse, *J. Fluid Mech.* **919**, A10 (2021).
- [21] G. Li, *J. Fluid Mech.* **934**, A20 (2022).
- [22] A. Farutin, M. Rizvi, W.-F. Hu, T. Lin, S. Rafai, and C. Misbah, *J. Fluid Mech.* **952**, A6 (2022).
- [23] A. Mikhailov and D. Meinköhn, *Lect. Notes Phys.* **484**, 334 (2007).
- [24] D. Boniface, C. Cottin-Bizonne, R. Kervil, C. Ybert, and F. Detcheverry, *Phys. Rev. E* **99**, 062605 (2019).
- [25] K. Lippera, M. Benzaquen, and S. Michelin, *Soft Matter* **17**, 365 (2021).



- [26] M. Sauzade, G. J. Ifring, and E. Lauga, *Physica D* **240**, 1567 (2011).
- [27] A. Farutin, O. Aouane, and C. Misbah, *Phys. Rev. E* **85**, 061922 (2012).
- [28] A. Farutin and C. Misbah, *Phys. Rev. Lett.* **110**, 108104 (2013).
- [29] B. J. Matkowsky and E. L. Reiss, *SIAM J. Appl. Math.* **33**, 230 (1977).
- [30] A. C. Fowler, *Mathematical Models in the Applied Sciences* (Cambridge University Press, Cambridge, UK, 1997).
- [31] C. N. Yang, *Phys. Rev.* **85**, 808 (1952).
- [32] I. Belykh, R. Kuske, M. Porfiri, and D. J. W. Simpson, *Chaos* **33**, 010402 (2023).
- [33] M. A. Teixeira and P. R. da Silva, *Physica D* **241**, 1948 (2012).